Nanometric summation architecture based on optical near-field interaction between quantum dots

Makoto Naruse, Tetsuya Miyazaki, and Fumito Kubota

National Institute of Information and Communications Technology, 4-2-1 Nukui-kita, Koganei, Tokyo 184-8795, Japan

Tadashi Kawazoe

Japan Science and Technology Agency, 687-1 Tsuruma, Machida, Tokyo 194-0004, Japan

Kiyoshi Kobayashi

Tokyo Institute of Technology, 2-12-1 Ookayama, Meguro-ku, Tokyo 152-8551, Japan

Suguru Sangu

Ricoh Co., Ltd., 16-1 Shinei-cho, Tsuzuki-ku, Yokohama, Kanagawa 224-0035, Japan

Motoichi Ohtsu

University of Tokyo, 7-3-1 Hongo, Bunkyo-ku, Tokyo 184-8795, Japan

Received July 22, 2004

A nanoscale data summation architecture is proposed and experimentally demonstrated based on the optical near-field interaction between quantum dots. Based on local electromagnetic interactions between a few nanometric elements via optical near fields, we can combine multiple excitations at a certain quantum dot, which allows construction of a summation architecture. Summation plays a key role for content-addressable memory, which is one of the most important functions in optical networks. © 2005 Optical Society of America

OCIS codes: 200.3050, 270.0270, 070.6020.

To meet future bandwidth requirements, a huge amount of computation must be performed at the nodes in optical networks and in data centers. Performing such computations in the optical domain[1] is expected to enhance overall system performance. However, integration of a large amount of optical hardware[2] is essentially constrained by the diffraction limit of light, which severly limits the overall capability.

Nanophotonics, on the other hand, is not restricted by the diffraction limit since it is based on local electromagnetic interactions between a few nanometric elements via optical near fields.[3] Consequently, suitable architectures should be built to exploit this capability of the physical layer. In this Letter we propose a data summation mechanism based on nanophotonics, which is, for instance, the basis for optical data matching or content-addressable memory (CAM).

We first describe architectural considerations regarding data matching and its optical implementation. CAM has an architecture in which the input signal content serves as a query to a database and the output is the address of data matching the input. CAM plays an important role in various applications, such as routers,[4] translation look-aside buffers, image processing, and data compression.

We can relate the CAM architecture to an inner product operation. We assume an N-bit input signal $\mathbf{S} = (s_1, \cdots, s_N)$ and reference data $\mathbf{D} = (d_1, \cdots, d_N)$. Here the inner product $\mathbf{S} \cdot \mathbf{D} = \sum_{i=1}^{N} s_i d_i$ will provide a maximum value when the input perfectly matches the reference data. The multiplication of two bits, namely, $x_i = s_i d_i$, has already been demonstrated by a combination of three quantum dots.[5] Therefore the key operation remaining is the summation $\sum x_i$, where all data bits x_i $(i = 1, \cdots, N)$ should be taken into account; this is shown schematically in Fig. 1(a). The existing ways of realizing such a data-gathering scheme include focusing lenses, optical waveguide couplings, and photodetector arrays; however, such methods impose yet another barrier to integration and miniaturization. In nanophotonics, on the other hand, optical energy is attracted to a certain quantum dot by optical near-field couplings between quantum dots, as described below.

The exclusiveness of the operations should be noted. The inner product $\mathbf{S} \cdot \mathbf{D}$ is, in fact, not enough to determine the correct matching of input $\mathbf{S}$ and reference $\mathbf{D}$; the inner product of the inverted input signal and reference data is also required. Inversion is, however, a difficult function to implement optically. One possible option is to properly design the modulation format,[6] for instance, by representing a logical level with two digits, for example, Logic 1 ="10" and Logic 0 ="01". Then, an N-bit logical input is physically represented by $2N$ bits, which makes the inner product equivalent to the matching operation. For the purpose of implementing the longest prefix matching, which is important for packet data transfer,[7] a "don't care" status is also required, and it can be coded as "11" in this scheme. Then, the resultant multiplication of a don't care bit to an incoming bit will be 1 for either Logic 0 or 1. Suppose that the reference data in memory $\mathbf{D}_1, \cdots, \mathbf{D}_M$ and input $\mathbf{S}$ are represented in the format described above. Then, the function of the CAM will be to derive the value j that maximizes $\mathbf{S} \cdot \mathbf{D}_j$ $(j = 1, \cdots, M)$.

In such a system each of the inner products is realized on the nanoscale, and therefore the overall CAM is realized in an extremely compact volume

0146-9592/05/020201-03$15.00/0

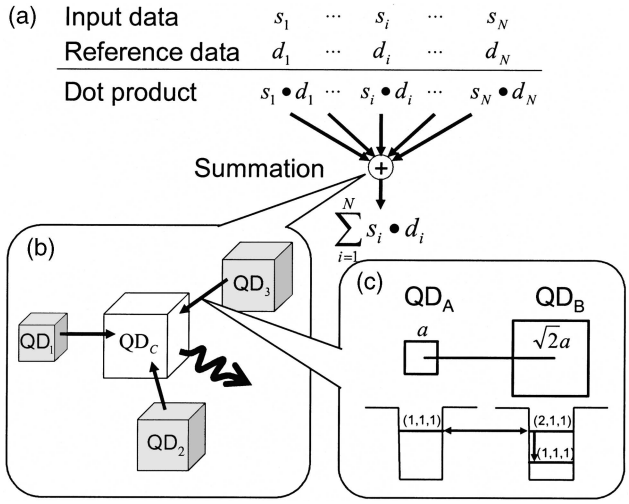

Fig. 1. (a) Inner product operation. (b) Summation mechanism in quantum dots. (c) Interdot interaction via an optical near field.

compared with its conventional counterpart. Moreover, conventional CAM VLSI chips consume lots of energy, whereas nanophotonic devices can be operated with extremely low energy.[5]

Here we describe the implementation of the summation architecture. It is based on interdot interaction via an optical near field, as shown schematically in Fig. 1(b) where excitations are transferred toward a certain quantum dot (QD_C at the center). As a fundamental case, we assume two quantum dots, QD_A and QD_B, as shown in Fig. 1(c). The ratio of the sizes of QD_A and QD_B is $1{:}\sqrt{2}$. There is a resonant quantized energy sublevel between these two dots, which are coupled by an optical near-field interaction.[5,8–10] Therefore the exciton population in the (1, 1, 1) level in QD_A is transferred to the (2, 1, 1) level of QD_B.[8–10] Note that this interaction is forbidden for far-field light.[9–11] Since the intrasublevel relaxation via exciton–phonon coupling is fast, the population is quickly transferred to the lower (1, 1, 1) level in QD_B. Similar energy transfers may take place in the dots surrounding QD_B among the resonant energy levels so that energy flow can occur. One could worry that, if the lower energy level of QD_B is occupied, another exciton cannot be transferred to that level because of the Pauli exclusion principle. Here, again because of the nature of the optical near-field interaction, the exciton population goes back and forth in the resonant energy level between QD_A and QD_B, which is called optical nutation.[9,10] Finally, both excitons can be transferred to QD_B. The lowest energy level in each quantum dot is coupled to a free photon bath to sweep out the excitation radiatively. The output signal is proportional to the (1, 1, 1)-level population in QD_B. Numerical calculations were performed based on quantum master equations in the density matrix formalism. The model Hamiltonian of the two dots is given by

$$H = \hbar \begin{bmatrix} \Omega_A & U \\ U & \Omega_B \end{bmatrix}, \tag{1}$$

where $\hbar U$ is the optical near-field interaction and $\hbar\Omega_A$ and $\hbar\Omega_B$ refer to the eigenenergies of QD_A and QD_B, respectively. For a two-exciton system we can prepare seven bases as summarized in Fig. 2(a), where one or two excitons occupy either one or two levels among the (1, 1, 1) level in QD_A (denoted by A), the (2, 1, 1) level in QD_B (denoted by B2), and the (1, 1, 1) level in QD_B (denoted by B1). These seven states are interconnected either by interdot near-field coupling (U), exciton–phonon coupling (Γ), or relaxation to the radiation photon bath (γ_A for QD_A and γ_B for QD_B). Within the Born–Markov approximation of the Liouville equation,[12,13] we can derive multiple differential equations. In the following we assume that $U^{-1} = 50$ ps, $\Gamma^{-1} = 10$ ps, $\gamma_A{}^{-1} = 2\sqrt{2}$ ns, and $\gamma_B{}^{-1} = 1$ ns as a typical parameter set.

First we consider an initial condition where there are two excitons in the system: one in QD_A and the other in QD_B (two-exciton system). The population of the (1, 1, 1) level in QD_B corresponds to the output signal, which is composed of three bases specified by (i), (ii), and (iii) in Fig. 2(a). The populations for those three bases, which are diagonal elements of the density matrix, are denoted by $\rho_{A,B1}(t)$, $\rho_{B1,B2}(t)$, and $\rho_{B1}(t)$, respectively; $\rho_{A,B1}(t)$ and $\rho_{B1,B2}(t)$ are related to

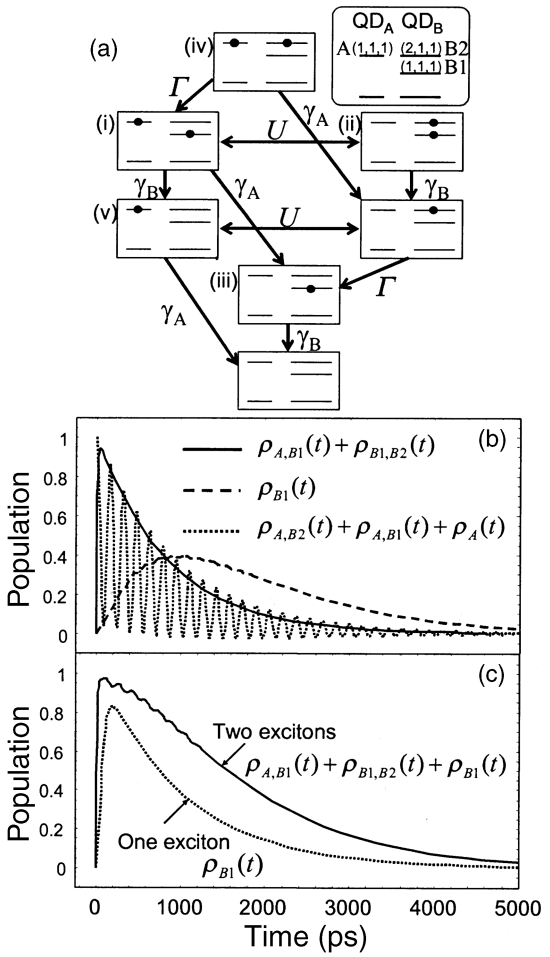

Fig. 2. (a) Bases of the two-exciton system in two quantum dots coupled by optical near fields. (b) Time evolution of the population in a two-exciton system. (c) Population comparison between one- and two-exciton systems.

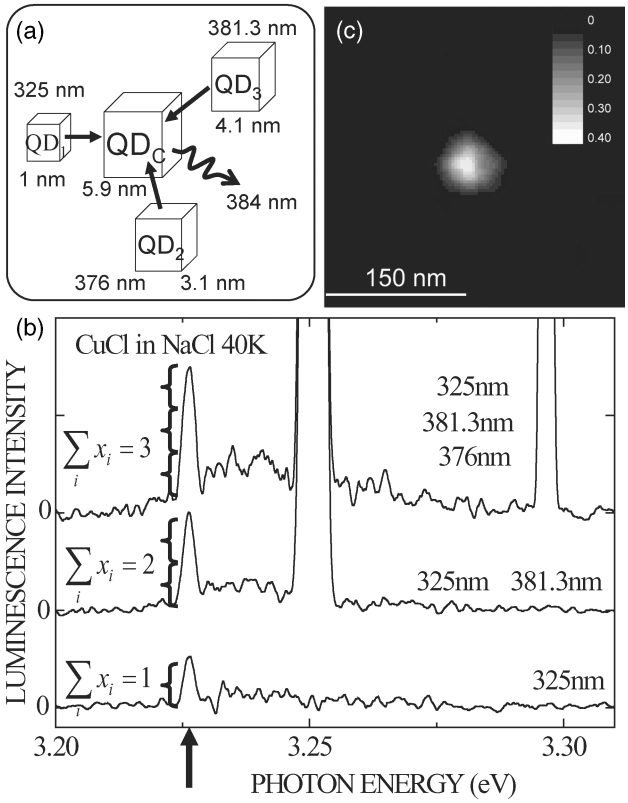

Fig. 3. Experimental results of the nanometric summation. (a) Quantum dot arrangement. (b) Luminescence intensity for three different numbers of excited QDs. (c) Spatial intensity distribution of the output photon energy.

two-exciton dynamics of the system. They show the time evolution of the one-exciton population in QD_A and in the upper level of QD_B, respectively, in addition to an exciton in the lower level of QD_B. The time evolution of $\rho_{A,B1}(t) + \rho_{B1,B2}(t)$ is shown by the solid curve in Fig. 2(b). The other population, $\rho_{B1}(t)$, has just one exciton in B1, and so it represents the output evolution of the one-exciton system, which is shown by the dashed curve in Fig. 2(b). Incidentally, the population when QD_A has an exciton, namely, the sum of the populations related to bases (i), (iv), and (v) in Fig. 2(a), is denoted by the dotted curve in Fig. 2(b). Nutation is observed as expected since the lower level of QD_B is likely to be busy and the interdot near-field interaction is faster than the relaxation bath coupling at each dot.

Next we compare the population dynamics between one- and two-exciton systems. The dotted curve in Fig. 2(c) shows the time evolution of the population in the lower level of QD_B, where, as initial conditions, one exciton exists only in QD_A. The solid curve in Fig. 2(c) is that for the two-exciton system. Physically the output signal is related to the integration of the population in the lower level of QD_B. Numerically integrating the population between 0 and 5 ns, we can obtain the ratio of the output signals between the two- and one-exciton systems as 1.86:1, which reflects the number of initial excitons, or the summation mechanism.

A proof-of-principle experiment was performed to verify the nanoscale summation using CuCl quantum dots in a NaCl matrix, which has also been employed for demonstrating nanophotonic switches[5] and optical nanofountains.[14] We choose a quantum dot arrangement in which small QDs (QD_1–QD_3) surrounded a large QD (QD_C), as shown schematically in Fig. 3(a). Here we irradiate at most three light beams with different wavelengths, 325, 376, and 381.3 nm, which excite QD_1, QD_2, and QD_3, respectively, with sizes of 1, 3.1, and 4.1 nm. The excited excitons are transferred to QD_C, and its radiation is observed by a near-field fiber probe. Notice the output signal intensity at a photon energy level of 3.225 eV in Fig. 3(b), which corresponds to a wavelength of 384 nm or a QD_C size of 5.9 nm. The intensity varies approximately as 1:2:3, depending on the number of excited QDs in the vicinity. The spatial intensity distribution was measured by scanning the fiber probe, as shown in Fig. 3(c), where the energy is converged at the center. Hence the architecture works as a summation mechanism based on exciton energy transfer via optical near-field interactions.

In summary, an architecture for data summation has been presented, and proof of principle has been demonstrated based on near-field coupling between quantum dots.

M. Naruse's e-mail address is naruse@nict.go.jp.

References

1. M. J. O'Mahony, D. Simeonidou, D. K. Hunter, and A. Tzanakaki, IEEE Commun. Mag. **39,** 128 (2001).
2. P. C. Teh, P. Petropoulos, M. Ibsen, and D. J. Richardson, IEEE J. Lightwave Technol. **19,** 1352 (2001).
3. M. Ohtsu, K. Kobayashi, T. Kawazoe, S. Sangu, and T. Yatsui, IEEE J. Sel. Topics Quantum Electron. **8,** 839 (2002).
4. H. Liu, IEEE Micro **22,** 58 (2002).
5. T. Kawazoe, K. Kobayashi, S. Sangu, and M. Ohtsu, Appl. Phys. Lett. **82,** 2957 (2003).
6. M. Naruse, H. Mitsu, M. Furuki, I. Izumi, Y. Sato, S. Tatsuura, M. Tian, and F. Kubota, Opt. Lett. **29,** 608 (2004).
7. K. Kitayama and M. Murata, IEEE J. Lightwave Technol. **21,** 2753 (2003).
8. T. Kawazoe, K. Kobayashi, J. Lim, Y. Narita, and M. Ohtsu, Phys. Rev. Lett. **88,** 067404 (2002).
9. S. Sangu, K. Kobayashi, A. Shojiguchi, T. Kawazoe, and M. Ohtsu, J. Appl. Phys. **93,** 2937 (2003).
10. S. Sangu, K. Kobayashi, A. Shojiguchi, and M. Ohtsu, Phys. Rev. B **69,** 115334 (2004).
11. Z. K. Tang, A. Yanase, T. Yasui, Y. Segawa, and K. Cho, Phys. Rev. Lett. **71,** 1431 (1993).
12. L. Mandel and E. Wolf, *Optical Coherence and Quantum Optics* (Cambridge U. Press, Cambridge, England, 1995).
13. H. J. Carmichael, *Statistical Methods in Quantum Optics I* (Springer-Verlag, Berlin, 1999).
14. T. Kawazoe, K. Kobayashi, and M. Ohtsu, in *Conference on Lasers and Electro-Optics (CLEO) 2004*, Vol. 96 of OSA Trends in Optics and Photonics Series (Optical Society of America, Washington, D.C., 2004), paper IFC1.